THE EFFECT OF IMPURITIES ON THE PERFORMANCE OF LITHIUM INTENDED FOR LITHIUM/THIONYL CHLORIDE BATTERY MANUFACTURE

W. P. HAGAN* and N. A. HAMPSON

Department of Chemistry, Loughborough University of Technology, Loughborough, Leicestershire LE11 3TU (U.K.)

R. K. PACKER

Admiralty Research Establishment, Portland, Dorset DT5 2JS (U.K.)

(Received October 22, 1987)

Summary

The elemental impurities in four different, commercially-available lithium samples have been determined. Cells consisting of these lithium samples as anodes and pressed acetylene black as cathodes were discharged at 20 °C and at 70 °C at a rate of 50 mA cm^{-2}. The passivating films remaining on the lithium surface after discharge were examined using electron microscopy and their elemental compositions determined using the surface sensitive technique of X-ray photoelectron spectroscopy. Performance characteristics (voltage and capacity) of test cells consisting, in part, of the different lithium samples are discussed in terms of impurity concentrations determined by secondary ion mass spectrometry and atomic absorption spectroscopy. The permeability and electronic conductivity of the LiCl passivating films are adduced as two possible reasons for the variations in capacity and on-load voltage of the different lithium samples.

Introduction

Except for the voltage delay phenomenon little attention has been paid to the performance of the lithium electrode in lithium–oxyhalide systems. We have recently become aware that not all lithium samples behave similarly in lithium–thionyl chloride ($Li/SOCl_2$) test cells. These performance differences may manifest themselves in lower load voltages or, in aggravated cases, lower capacities. In cases where the cells have a lower capacity, despite their being designed to be cathode limited, they are obviously anode limited. It is usual to expect that provision of excess lithium and electrolyte solution will ensure a cathode limited configuration. Visual examination of cells

*Author to whom correspondence should be addressed.

0378-7753/88/$3.50 © Elsevier Sequoia/Printed in The Netherlands

discharged to a point where it was obvious that one or more individual cell components had failed showed that lithium and the electrolyte were still present in excess, and earlier data showed that similarly formulated and discharged cathodes had higher capacities. The fact that lower capacities were invariably associated with lower load voltages suggested that film formation on the lithium surface was somehow attenuating the supply of Li^+ ions to the electrolyte solution. Similar behaviour has been recorded with certain lithium alloys, notably Li/Cd and Li/Mg (5 at.%) [1], but the same work also showed that it was perfectly feasible to alloy lithium with a range of other metals without any deleterious effects.

James [2, 3] reported the anodic passivation of Li in 1.5 M $LiAlCl_4/SOCl_2$ electrolyte solutions. He emphasised that the anodic passivation was distinct from the chemically formed LiCl passivating layer which is responsible for the voltage delay effect. He ascribed this anodic passivation to the formation of a discrete film on the Li surface. A tentative suggestion, that passivation was due to the enrichment and consequent precipitation of $LiAlCl_4$, was offered.

A lithium chloride film is formed on a lithium surface when it is allowed to contact an $LiAlCl_4/SOCl_2$ solution. This lithium chloride film has a dual configuration. The first layer, which is in intimate contact with the lithium surface, is formed immediately the lithium contacts the electrolyte solution [4]. This inner layer of lithium chloride is highly resistive (10^7 - 10^8 Ω cm [4]), and even during corrosion and anodic dissolution a breakdown and repair mechanism ensures the perpetuation of the film [5]. The presence of this so called α layer [6] is thought to be responsible for the long shelf-life of $Li/SOCl_2$ batteries as it is instrumental in preventing complete dissolution of the lithium anode by the highly aggressive electrolyte solution. The second layer, the β layer, which grows continuously on the first one, is much thicker, about 50 μm, and is non-insulating in nature because it is porous and highly defective [7].

On discharge (anodic polarisation) Li^+ migrates through the α layer, only several molecular layers thick, since the film is essentially LiCl which is an Li^+ ionic conductor [8]. The Li^+ ions are then free to migrate through the pores and channels of the porous outer layer which is thought to be progressively eliminated by mechanical and thermal degradation [8]. The initial anodic dissolution of Li is thought to be highly localised, occurring at pinholes and other imperfections in the protective film [9]. The film is eventually dislodged mechanically or fractured when sufficient lithium has been dissolved underneath the film. It has been shown that it is the thickness and morphology of this film which controls the voltage delay characteristics of the system [9].

We undertook this study in the belief that even trace amounts of a particular impurity, or combination of impurities, present in the lithium could affect the thickness and growth mechanisms of either film, α or β, which could have a profound effect on the discharge characteristics of a cell utilising that lithium. The presence of Fe^{3+} or Fe^{2+} is thought to accelerate

the growth of the solid electrolyte interphase (SEI) [5], which is essentially the α film, with or without the presence of the β film, which if it is present may comprise a highly porous, open-structured film or a mechanically strong, low porosity layer. The SEI is commonly in the region of 10 - 1000 Å thick, and the secondary, more porous film is tens of μm thick [5]. Doping the SEI with foreign ions such as Fe^{2+}, Fe^{3+}, or Al^{3+}, from high concentrations of $LiACl_4$ in $SOCl_2$, would cause a significant increase in the electronic conductivity of the SEI. The growth rate of the SEI in $LiAlCl_4/SOCl_2$ solutions was found to increase with the $LiAlCl_4$ concentration [10].

That the implantation of suitable impurity ions in the SEI can increase the electronic conductivity is well documented [5] and, in so doing, it can affect the thickness and growth rate of the film. The thickness of the SEI is regulated by the electron-tunnelling range [5] which is a function of the electronic conductivity of the layer. The rate of growth of the film is determined by the rather low ionic conductivity of the solid electrolyte interphase (LiCl), as the rate-determining step is ionic transport through the SEI [11].

As we were concerned with the voltage and capacity of $Li/SOCl_2$ cells where the LiCl passivating film controls Li^+ transport, we addressed ourselves to a study of the morphology and elemental composition of the LiCl film present after discharge, this being considered to best represent the film conditions responsible for premature cell failure or decreased load voltage. We used two techniques, X-ray photoelectron spectroscopy and electron microscopy to study the composition and morphology of the LiCl film on anodes from discharged $Li/SOCl_2$ cells. Secondary ion mass spectrometry was employed for the bulk analysis of the Li samples in order to survey rapidly an extensive mass number range. Initially this was invaluable as the nature of the impurities sought was unknown, and the technique's sensitivity (ppm–ppb) and accuracy when comparing similar samples was adequate for our purposes.

Experimental

The lithium samples used were discharged in a PTFE sandwich-type cell construction shown schematically in Fig. 1. The carbon cathode, which was backed by a nickel current collector, was prepared from 50% compressed Shawinigan Acetylene Black (SAB) with 5% w/w PTFE dispersion as binder. The PTFE dispersion was slurried into the SAB with propan-2-ol and dried in an oven at 90 °C. The mixture, after powdering, was pressed at moderate pressures to form mechanically strong cathodes without the requirement for metal meshes for additional support. The separator was a layer of ceramic cut to suitable size. Anodes were cut to the same size as the carbon cathodes (2.4 cm^2) with metal punches. These discs were then pressed onto a length of nickel mesh (Ni 200, Expanded Metal Company) which provided electrical contact. The separate cell components were then sandwiched together in the

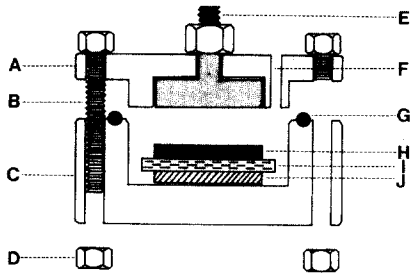

Fig. 1. PTFE test cell for lithium–oxyhalide systems. The cell is composed of : A, PTFE upper section; B, assembly bolt; C, PTFE lower well; D, retaining nut; E, nickel current collector stud; F, sealable filling port; G, Viton sealing ring ("O" ring); H, carbon cathode; I, ceramic separator paper; J, lithium anode.

PTFE cell, the two halves of which were connected by steel bolts which were tightened to a constant torque to give the same load conditions for each discharge.

The cell was filled to overflowing with a 1.8 M solution of $LiAlCl_4$ in $SOCl_2$. Puriss-grade $SOCl_2$ (Fluka) and as-received Fluka purum-grade $AlCl_3$ and LiCl were used. Once opened, reagents were stored and weighed in dry air, <0.1% (20 °C) relative humidity.

The lithium samples originated from four sources; Lithco (Lithium Corporation of America), Ventron GmbH, Foote Mineral, and Fluka AG. The Lithco sample was 99.9% Li minimum (Battery Quality), the Ventron sample was 99.9% Li, the Foote sample was 99.9% Li (Battery Quality), and the Fluka lithium sample was supplied in powder form (50 - 200 μm) alloyed with 0.5% w/w sodium. The Fluka sample was prepared for use in the cell by melting the powder in a platinum crucible in dry argon and casting in nickel boats prior to rolling to a foil for use in the cell. Identical performance could be obtained from the lithium by pressing the powder in a die at 350 kgf cm^{-2} to yield lithium discs of the desired thickness which could then be punched to size.

The cells were discharged at constant current by means of a potentiostat used in a galvanostatic mode and the discharge curves were output to a Y–t strip recorder. All cells were discharged at 50 mA cm^{-2} and at 20 °C and 70 °C. The elevated temperatures were maintained in a thermostatted, electrically heated, glass pressure vessel into which the cells were placed. Test runs, during which the internal cell temperature was measured using a glass-encapsulated, platinum bead thermistor, established that thermal equilibrium was attained in <20 min.

All cells were discharged to 2.5 V, whereupon they were immediately dismantled and the lithium electrode washed in three 10 cm^3 portions of pure $SOCl_2$ to remove $LiAlCl_4$ from the mainly LiCl surface film. After thorough drying the samples were stored in glass containers with metal screw caps and an inner rubber seal. We have established on a number of previous occasions that these containers are suitable for the transfer of moisture sensitive materials between different dry-box sites. Samples in-

tended for scanning electron microscopic (SEM) analysis were mounted on aluminium sample studs using an electrically conductive cement.

Sample transfer to the electron spectrometer for the X-ray photoelectron spectroscopic (XPS) studies was effected via a dry-box handling port attached to the entry air lock of the instrument. The Al Kα X-ray line (1486 eV) was used as the excitation source and the area analysed was 0.4 cm^2. An argon ion gun (10 keV) was available for sample cleaning and depth profiling. Compositions of the LiCl films were obtained using experimentally determined relative sensitivity factors derived from chemical standards. Absolute concentrations must be considered approximate (errors are typically about 10%) although accurate comparisons may be made between similar samples.

The SEM (scanning electron microscope) studies on the discharged lithium were performed without the need to apply any conductive coating such as vapour-deposited Al or Au, which is the usual practice for non-conducting materials such as Al_2O_3. The film must therefore have been rendered sufficiently conductive to avoid surface charging by defects in the film probably caused by the presence of impurities. At all stages extreme care was exercised to ensure that the samples never came into contact with anything other than an atmosphere of $<0.5\%$ (20 °C) relative humidity.

The polarisation of the lithium anode was recorded in a cell similar to that shown in Fig. 1, except that provision was made for the insertion of an Ag:AgCl reference electrode through the cell wall so that it was sited between the anode and the cathode. The reference, made by the anodic polarisation of Ag wire in dilute HCl, was held between two discs of the ceramic separator, this being held between the carbon and lithium so that while all three electrodes were as close as possible to each other they were unable to come into electrical contact except via the electrolyte solution. The reference, although perfectly stable over a number of polarisation experiments, was cleaned and freshly plated with AgCl as a precaution after each discharge.

A quantitative analysis of Ca, Na, K, Si, Sn, Al, and Fe was carried out using either atomic absorption (AA) or inductively coupled plasma spectrometry (ICP). The lithium samples to be analysed were initially dissolved in methanol and then in triply-distilled water. Standard solutions were matrix matched with high purity LiCl (AA standard) to counter any interferences lithium might have had on the determinations. Ca, Na, K, and Fe were determined by AA while Si, Sn, and Al were determined by ICP.

Secondary ion mass spectra (SIMS) of the lithium metal samples were recorded but, although SIMS has a sensitivity in the ppm to ppb range, it was not possible to compare quantitatively different absolute elemental concentrations in a sample because of differing ion yields. For the same elements in different samples in the same matrix the comparative concentrations are very accurate. So although absolute concentrations must be determined from an external Standard, with known concentrations of the elements of interest, the technique is quantitative for homogeneous systems

and has a linear dependence of signal-to-concentration for dilute systems. Thus, the analysis of impurity levels in lithium metal lends itself to this technique, since absolute impurity concentrations may be determined in a Standard, albeit with some difficulty, by other, more common, analytical methods such as AA and ICP.

Results and discussion

Scanning electron microscopy (SEM)

Electron photomicrographs of the lithium anodes discharged at 20 °C and at 70 °C are shown in Fig. 2. The surface of an undischarged lithium

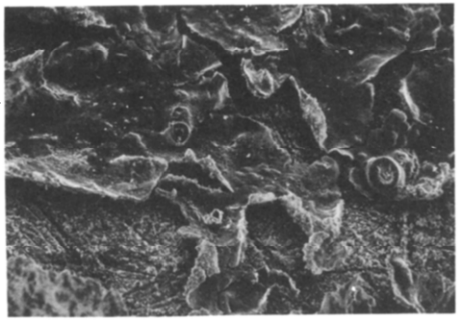

(a)

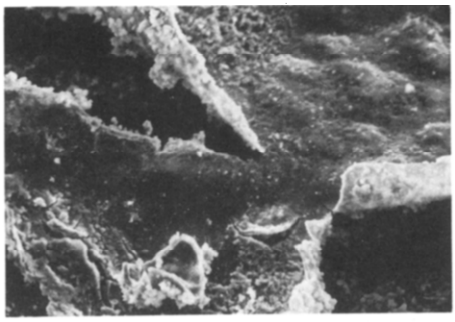

(b)

(c)

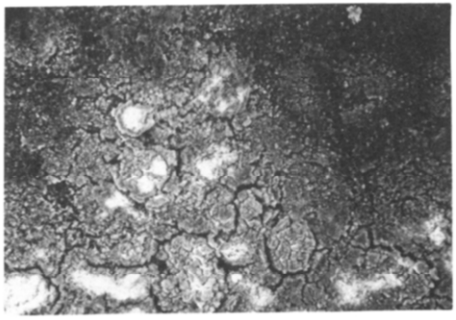

(d)

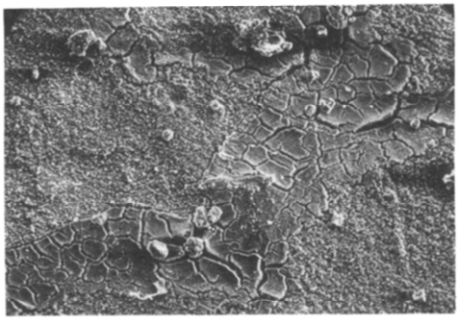

(e)

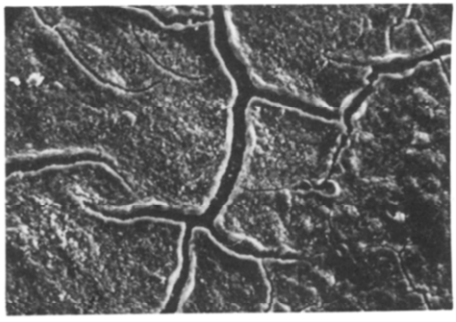

(f)

(continued)

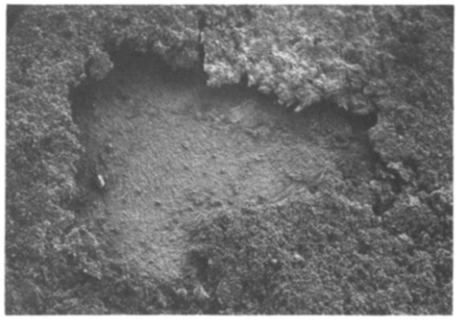

(g)

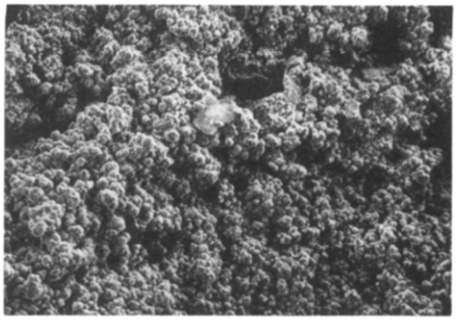

(h)

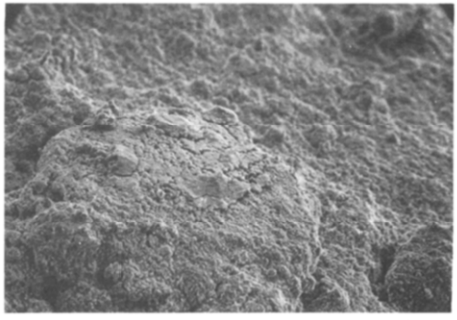

(i)

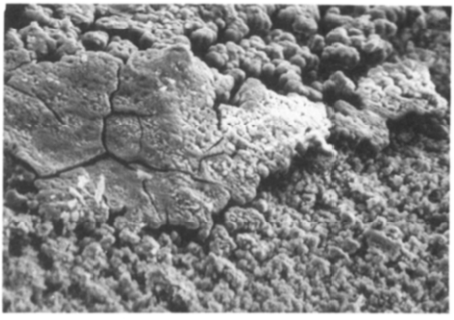

(j)

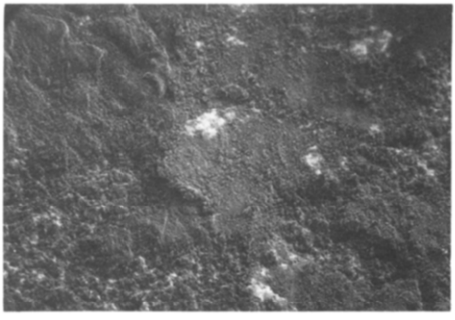

(k)

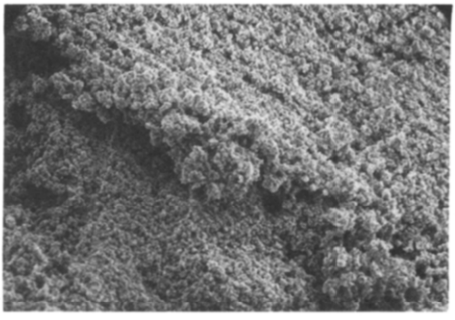

(l)

Fig. 2. SEM photomicrographs of lithium surfaces after discharge at 20 °C and at 70 °C. (a), (b) Lithco lithium discharged at 20 °C (200× (a) and 1000× (b) magnification); (c), (d) Fluka lithium discharged at 20 °C (200× (c) and 1000× (d) magnification); (e), (f) Ventron lithium discharged at 20 °C (200× (e) and 1000× (f) magnification); (g), (h) Lithco lithium discharged at 70 °C (200× (g) and 1000× (h) magnification); (i), (j) Fluka lithium discharged at 70 °C (200× (i) and 1000× (j) magnification); (k), (l) Ventron lithium discharged at 70 °C (200× (k) and 1000× (l) magnification). All photomicrographs reduced by 9/20 (45%) in reproduction. Cells discharged at 70 °C were in contact with the electrolyte solution for 30 min before discharge which allowed time for them to attain thermal equilibrium. The cells discharged at 20 °C were stored similarly to allow for film growth at that temperature before discharge.

anode is relatively smooth with very little roughening. The Lithco samples at both 20 °C and 70 °C exhibit a high degree of modification to the chemically-formed passive layer. At 70 °C the layer is heavily cratered and these expand by undermining the passive layer. The tendency to form craters at 20 °C is less marked; instead there is a spalling off of the surface layer to reveal what is essentially the metal surface covered with crystallites of, presumably, lithium chloride.

At 20 °C the Ventron and Fluka lithium samples show fissuring of the chemically-formed layer, but to a much lesser extent than with the Lithco sample. At 70 °C the LiCl films on the Ventron and Fluka surfaces appear to be much more porous than at 20 °C, as with the Lithco sample, but there is no clear evidence for crater formation.

The Lithco sample shows the most disruption of the passivating layer, both at 20 °C and at 70 °C, while the passivating layer for all the samples discharged at 70 °C is much more porous than for those discharged at 20 °C.

Anode polarisation

The anodic polarisation curves presented in Fig. 3 are mainly ohmic in nature, reflecting the mobility of Li^+ ions through the chemically-formed passivating layer. Clearly, at low rates, <5 mA cm^{-2}, the differences, while detectable, might not be significant when compared with discharge rates of >100 mA cm^{-2}.

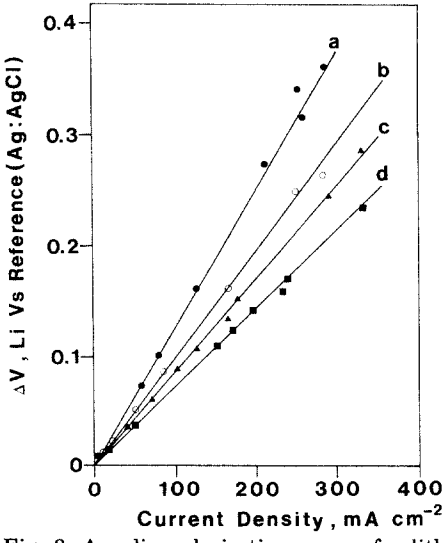

Fig. 3. Anodic polarisation curves for lithium anodes in a 1.8 M $LiAlCl_4/SOCl_2$ electrolyte solution with SAB cathodes. All polarisation measurements were recorded at 70 °C. The polarisation of the lithium anode was measured relative to an Ag:AgCl reference electrode. Curve a is the polarisation curve for the Ventron lithium sample, curve b for the Foote sample, curve c for the Fluka sample, and curve d for the Lithco sample. All samples were in contact with the electrolyte solution for precisely 30 min before the polarisation measurement was made. This was necessary for the cell to achieve thermal equilibrium.

The polarisation curve with the shallowest gradient belongs to the Lithco sample, the others being represented by progressively steeper polarisation curves corresponding to lithium samples with passivating layers which offer greater resistance to the mobility of Li^+ ions. These polarisation curves are a sensitive test of a particular anode's performance characteristics and the results obtained here are in complete accord with the discharge results.

X-ray photoelectron spectroscopy (XPS)

A low resolution, broad energy XPS spectrum of a lithium anode discharged at 20 °C at the 50 mA cm^{-2} rate is shown in Fig. 4. The anode surface after discharge was only exposed to the electrolyte solution for about 60 s, as the cell design permitted rapid disassembly and removal of components. Further unavoidable exposure to the glove box atmosphere and to the less-than-ultra-high-vacuum atmosphere in the entry port of the electron spectrometer followed during transfer procedures. The XPS technique probes only the top 25 - 50 Å of the surface and this, unfortunately, cannot be considered to be completely representative of the anodically-formed passive film created during discharge. The variable amounts of carbon present on the surface (in the form of hydrocarbons) is a contaminant frequently encountered in XPS studies. The elemental compositions of the passive films are quoted in at.% (Tables 1 and 2). They are determined from the area under each XPS peak with corrections made for such factors as the electron's mean free path, the photoionization cross section, and the energy dependence of the hemispherical analyser. The results are not strictly quantitative but provide an estimate (to within 10%) of the passive layer's composition before and after discharge.

The two most significant elemental changes in the anodes stored and discharged at both 20 °C and at 70 °C are the tin and silicon levels. "Stored" in this sense means that the anode was equilibrated at the appropriate temperature for the same length of time as an anode under discharge would be in contact with the electrolyte before dissassembly and washing. The

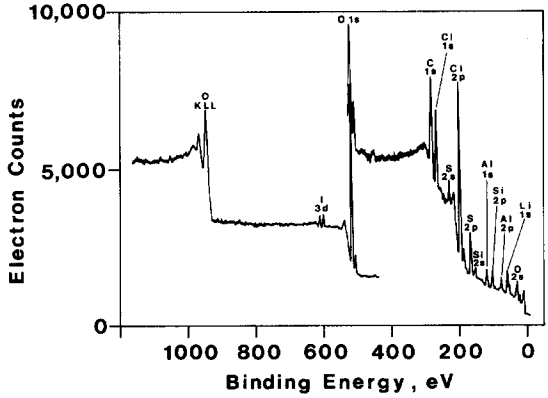

Fig. 4. Low resolution, broad energy, XPS spectrum of a lithium anode (Ventron) discharged at 20 °C at the 50 mA cm^{-2} rate.

TABLE 1

Surface compositions of the LiCl passivating film as determined by XPS
Lithium samples were stored and discharged at 20 °C and at 70 °C with 1.8 M $LiAlCl_4$ in $SOCl_2$.

Lithium sample	Elemental concentration (at.%)							
	Si	S	C	Sn	I	Zn	Ca	Na
Lithco stored 20 °C	1.0	0.6	13.3	—	—	—	—	—
Ventron stored 20 °C	0.8	5.1	15.2	—	0.2	—	—	—
Fluka stored 20 °C	2.2	—	58.1	—	—	—	—	—
Lithco stored 70 °C	0.7	0.9	2.5	—	—	—	—	—
Ventron stored 70 °C	1.0	8.3	4.5	—	0.4	1.1	0.8	—
Fluka stored 70 °C	3.4	—	14.5	—	—	—	—	0.5
Lithco discharged 20 °C	4.8	0.6	17.1	0.4	—	—	—	—
Ventron discharged 20 °C	2.5	2.9	14.6	< 0.005	0.2	—	—	—
Fluka discharged 20 °C	2.2	0.8	19.0	0.2	—	—	—	—
Lithco discharged 70 °C	2.7	0.4	16.0	0.3	—	—	—	—
Ventron discharged 70 °C	2.6	1.3	18.4	0.3	—	—	—	—
Fluka discharged 70 °C	3.6	2.9	16.2	< 0.005	—	—	—	—
Lithco difference 20 °C	+3.8	no change	+3.8	+0.4	—	—	—	—
Ventron difference 20 °C	+1.7	−2.2	−0.6	+0.05	no change	—	—	—
Fluka difference 20 °C	no change	+0.8	−39.1	+0.2	—	—	—	—
Lithco difference 70 °C	+2.0	−0.5	+13.5	+0.3	—	—	—	—
Ventron difference 70 °C	+1.6	−7.0	+13.9	+0.3	−0.4	−1.1	−0.8	—
Fluka difference 70 °C	+0.2	+0.5	+1.7	+0.05	—	—	—	−0.5

TABLE 2

Composition of "as-received" lithium
A form of depth profile is achieved with argon ion sputtering. A 31 min sputtering time etches the surface to approximately 120 Å.

Etch time (min)	Elemental concentration (at.%)							
	Li	S	Cl	C	O	Na	Sn	Lithium sample
0	40.0	2.7	41.4	6.1	9.7	—	—	Lithco
6	43.3	7.9	8.1	3.1	37.6	—	—	Lithco
16	67.1	1.3	1.3	5.6	24.0	—	—	Lithco
31	67.1	0.5	0.4	6.9	23.9	—	—	Lithco
0	35.6	3.3	7.3	18.0	35.9	—	—	Ventron
2	54.7	1.7	9.6	1.2	32.8	—	—	Ventron
6	59.9	0.8	9.5	0.9	28.9	—	—	Ventron
16	70.9	—	5.9	—	23.2	—	—	Ventron
31	71.3	—	2.6	—	26.1	—	—	Ventron
0	37.0	1.5	33.4	12.0	15.5	0.4	0.1	Fluka
2	43.1	1.1	35.4	2.6	17.5	0.3	0.2	Fluka
6	52.1	1.1	21.5	—	24.7	0.4	0.2	Fluka
16	62.1	0.8	15.4	—	21.3	0.3	0.1	Fluka
31	64.9	0.5	9.9	—	22.1	0.7	—	Fluka

XPS analysis of the lithium samples (Table 2) which had not contacted the electrolyte solution showed no Si present and only Sn in the Fluka sample. The lithium samples stored at 20 °C and at 70 °C (Table 1) showed the presence of Si in the LiCl film and no Sn. The ceramic separator contained a small amount of silica as stabiliser, but storage of lithium in the electrolyte solutions at both 20 °C and 70 °C in the absence of separator showed comparable Si levels. These, therefore were not considered to be due to the diffusion of Si from the ceramic. A discussion of Si 2p binding energies and the identification of Si from the ceramic is discussed below.

At both temperatures the Fluka sample showed virtually no change in Si levels after discharge. The LiCl films formed under storage conditions at 20 °C and at 70 °C were devoid of Sn but, after discharge, all the samples at both temperatures showed an increase in Sn level to varying degrees. The ionic radii of Sn^{4+} and Li^{+} are 0.71 and 0.60 Å, respectively, so they are probably equally mobile in the outer, porous β LiCl layer. A corollary of Sn^{4+} being present in the β layer is that it must be able to permeate the SEI as it originates from the bulk of the lithium sample. The presence of S and Cl on the fresh lithium samples (Table 2) is due to contact with $SOCl_2$ vapours in the glove box. That the so-formed LiCl film is very thin was confirmed by sputtering the surface *in situ*. After 31 min of sputtering the Cl and S concentrations fall significantly.

The fall in concentration of Cl and S in the analysis area after 31 min of sputtering is suggestive of a film some 100 - 120 Å thick. The C and O levels

are due to atmospheric contamination, the C being easily removed by sputtering. The O levels appear to be almost constant in the penetration depths studied and it is probably present as Li_2O throughout the metal.

The measured binding energies suggest that the Sn 3d peak at 486.8 eV is due to $SnCl_4$, while the Si 2p peak could be resolved into two bands at 101.2 and 102.6 eV. The binding energy of the Si 2p peak in silica (measured from the ceramic) was 102.8 eV, which clearly takes account of the 102.6 eV band in the LiCl film. The band at 101.2 eV, which does not originate from the separator, is possibly organic in nature (Ph_4Si, Ph_3Si, and $Ph_3SiOSiPh_3$ [12]), or the chloride, which seems the more likely of the two. Like Sn, the Si levels have increased in the samples after discharge, the exception being the Fluka sample which shows little or no change. Si^{4+} has an ionic radius of 0.41 Å, which suggests a mobility through the SEI equal to, or better than, Li^+.

Neither Sn nor Si was found in a sample of electrolyte evaporated to dryness — essentially $LiAlCl_4$ plus impurities concentrated from the original $SOCl_2$ sample. No Sn was found in the ceramic separator.

Iodine which could only be identified on certain Ventron lithium samples had an I 3d binding energy of 618.8 eV which is suggestive of the presence of LiI in the passive film. The S 2p peak in the Fluka samples discharged at 20 °C and at 70 °C was clearly resolved into two components with binding energies of 163.9 and 169.9 eV, corresponding to ionizations from elemental S and sulphate, respectively. An XPS study of Li/SO_2 cell anodes identified Li_2SO_4 in the lithium passive film of both discharged and undischarged cells [13]. It is possible that the presence of LiI in the passive layer has oxidised SO_2, produced in the reduction of $SOCl_2$ to Li_2SO_4, in a manner analogous to the decomposition of SO_2 by LiBr [14]

$$4LiI + 4SO_2 \longrightarrow 2Li_2SO_4 + 2I_2 + 2S \quad (1)$$

Zinc as a chloride or sulphide (binding energy 1022.1 eV) and calcium as sulphate (347.6 eV) were identified on the sample of Ventron lithium stored in the electrolyte solution at 20 °C and not discharged. These two elements were not found in any other sample.

A similar XPS analysis of the LiCl film [15] on lithium samples discharged at 1 mA cm^{-2} (10% discharge) showed that the major constituents of the film were lithium and chlorine with substantially smaller quantities of sulphur, carbon, and oxygen. Silicon, with a trace of sulphur [7], has been found in undischarged films by means of X-ray energy dispersive analysis (EDAX).

Secondary ion mass spectrometry (SIMS)

A depth profile analysis for Li, Na, Ca, Si, K, and Fe is shown in Fig. 5. Depth profiling monitors selected species sequentially as a function of time as the sample surfaces are eroded by oxygen ion sputtering. Molecular ions with the same mass number could contribute to the mass spectrum but, fortunately, complex molecular ions have a narrower energy distribution

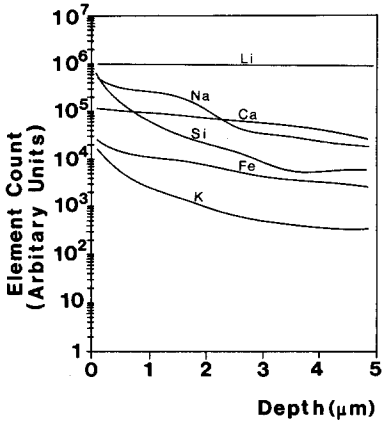

Fig. 5. Depth profile (SIMS) of a fresh lithium sample (Fluka). The arbitrary ordinate scale is derived from the number of counts recorded according to the atomic ions detected after mass analysis.

than atomic species and may be discriminated against if higher energy ions alone, above 100 eV, are used to form the mass spectrum. Most of the elements show a slight surface excess concentration, but this rapidly disappears and the depth profiles plateau as the surface layers are sputtered away.

The basic equation for quantitative SIMS can be written:

$$N_A = \text{const.}\, S_A \phi\pm \cdot C_A \qquad (2)$$

where N_A is the current of detected particles of mass A, S_A the respective sputtering rate, and C_A the concentration of component A [16]. The constant contains primary current and apparatus transmission parameters. The most significant factor in eqn. (2) is $\phi\pm$, the ionization probability, which is strongly dependent on the sputtered species and on the work function at the surface. This may vary between 10^{-5} and 10^{-1} for different atoms and surface conditions. This is a strong limitation on quantitative SIMS but the spread in $\phi\pm$ can be minimised by using oxygen primary ions for sputtering, as in this work, which increases the ionization probability for positive secondary ions and stabilises the surface state [17]. The change in S_A is generally smaller (within one order of magnitude) [18].

Table 3 lists the relative intensities (normalised to lithium) for the seven elements mass analysed in the depth profile analysis. The results of the wet chemical analysis in Table 4 correlate with the relative ion yields found by SIMS. In addition to the elements found in Table 3, traces (<0.000 01 wt.%) of Sr and Ba were detected by SIMS in all the lithium samples. The Fluka sample also had Ti, P, Cu, and Zn present between 0.000 01 and 0.0001 wt.%. These elements were not determined so precisely as the others, as their exclusion from the other samples rendered a precise knowledge of their exact concentrations relatively unimportant.

TABLE 3

Relative secondary ion yields for the lithium metal samples tested
The ion current N_x for the element X is given relative to a lithium ion current N_{Li} of unity.

	Ion current relative to Li N_x/N_{Li}								
Source	Ca	Na	K	Sn	Mg	Al	Fe	I	Si
Lithco	3×10^{-4}	5×10^{-4}	3×10^{-5}	1×10^{-6}	5×10^{-6}	1×10^{-6}	1×10^{-6}	—	4×10^{-6}
Foote	1×10^{-3}	5×10^{-3}	2×10^{-6}	1×10^{-6}	1×10^{-5}	1×10^{-6}	1×10^{-6}	—	1×10^{-6}
Ventron	2×10^{-3}	7×10^{-3}	4×10^{-5}	2×10^{-6}	7×10^{-6}	1×10^{-6}	5×10^{-5}	—	1×10^{-6}
Fluka	5×10^{-2}	3×10^{-2}	4×10^{-4}	2×10^{-4}	1×10^{-2}	3×10^{-2}	4×10^{-3}	—	6×10^{-3}

TABLE 4

Impurity concentrations (by element) in wt.% for the four lithium samples evaluated
The wet chemical analyses were carried out using a combination of AA and ICP.

	Elemental composition (wt.%)								
Source	Ca	Na	K	Si	Sn	Al	Fe	I	Cl
Lithco	0.00004	0.001	0.009	0.001	0.0002	0.001	0.0006	—	0.001
Foote	0.0008	0.004	0.001	0.001	0.0003	0.001	0.0006	—	0.001
Ventron	0.0008	0.005	0.007	0.001	0.0003	0.001	0.0008	—	0.002
Fluka	0.0010	0.49	0.09	0.05	0.03	0.008	0.07	—	0.002

Discharge results

The discharge results are shown in Figs. 6 and 7, but in isolation they provide no indication of the causes of the premature failure of some of the cells. Considered with some of the previously presented results, however, they demonstrate that cell failure cannot always be attributed to LiCl blocking the carbon electrode. The work by James [2, 3] did not consider the effect of utilising different Li samples on the anodic passivation times and we assume that, as all the other cell components were invariant, the presence of impurities in certain of the Li samples was responsible for the observed lower load voltages and capacities. The different load voltages correlate with the polarisation results (Fig. 3), as would be expected, while the different discharge times do not appear to be necessarily related to the ordering of load voltages. Examination of Tables 3 and 4 reveals that the ordering of discharge times is related to the impurity concentration of sodium in the sample, there being a significant decrease in discharge time for the Fluka sample (0.5% w/w Na) at 70 °C. It has long been regarded as

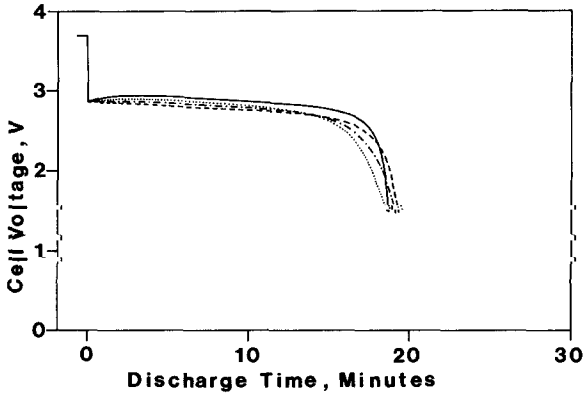

Fig. 6. Discharge curves recorded for the various lithium samples tested at 20 °C at the 50 mA cm^{-2} rate with 1.8 M $LiAlCl_4$ in $SOCl_2$. ——, Lithco sample; — — —, Ventron; ·····, Fluka; — · —, Foote lithium.

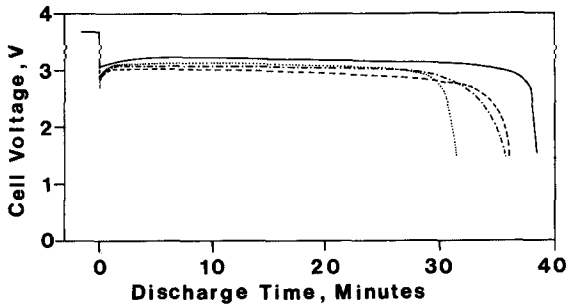

Fig. 7. Discharge curves recorded for the various lithium samples tested at 70 °C at the 50 mA cm^{-2} rate with 1.8 M $LiAlCl_4$ in $SOCl_2$. ——, Lithco sample; — — —, Ventron; ·····, Fluka; — · —, Foote lithium.

desirable to minimise sodium concentrations in lithium intended for battery manufacture, and its deleterious effect on discharge times is well illustrated in the cells discharged at 70 °C. Saturating the electrolyte solution with NaCl has no effect on the discharge times [19] for any of the lithium samples investigated, demonstrating that the effect is only exerted by sodium metal present in the anode.

The different, but quite reproducible, load voltages are not so easily explained. The Fluka sample had the highest concentration of any of the impurity elements analysed, but it did not exhibit the lowest voltage on load. It has been reported that there is a voltage penalty associated with the use of Li–Si and Li–Al alloy anodes in organic electrolyte cells [20] but, as the levels found in both the wet chemical and the SIMS analyses do not correlate with the measured on load voltages, we consider the Si and the Al concentrations to be below the level at which they would have an effect on the voltages.

We assume the voltage losses to be due to the conductivity of the LiCl passivating layer (SEI). The growth rate and morphology of this film may be influenced by impurities, or a combination of impurities, which we did not detect. The Fluka sample had the highest impurity levels of any of the lithium samples tested and it is somewhat surprising that it has such a high on load voltage on test. We assume that the high impurity levels, of Sn in particular, persist into the SEI, markedly increasing the electronic conductivity [5].

Recent work [21] indicated that Fe present in solution and stored in contact with lithium anodes at ambient temperature for over 4 weeks increases the voltage delay in $Li/SOCl_2$ cells with 1.5 M $LiAlCl_4$ as the supporting electrolyte. It is thought that Fe in solution is reduced onto the lithium metal surface to become catalytic sites for the rapid reduction of $SOCl_2$ and generate excess LiCl. Reference 21 quotes a 10× reduction in discharge time (to a predetermined voltage cut-off of 2.7 V at a discharge current density of 6 mA cm^{-2}) when 70 ppm of Fe was added to the catholyte (1.5 M $LiAlCl_4/SOCl_2$). The on-load voltage dropped from 3.24 V to 2.85 V, reflecting the thickness of the LiCl passivating film.

Our results for storage times of <20 min at room temperature and at 70 °C in Figs. 6 and 7 show that at both temperatures the lithium sample with the highest Fe concentration (Fluka) does not have the lowest on-load voltage. The discharge times at room temperature are approximately equal, and at 70 °C the Fe concentration does not correlate with discharge time. We suspect that Fe present in the lithium anode has little or no influence on the growth kinetics of the LiCl passivating film when compared with Fe in solution in the catholyte. Although our storage times were much shorter than the 4 weeks of ref. 21 we still find it impossible to correlate on-load voltages and discharge times with Fe levels in the lithium anode. Of the other impurities present in the Fluka lithium, Ca^{2+} and K^+ have ionic radii of 0.99 and 1.33 Å, respectively, rendering them too large to be transported through the SEI. Only the ionic radii of Sn^{4+} (0.71 Å), Mg^{2+} (0.65 Å), Al^{3+} (0.50 Å),

and Si^{4+} (0.41 Å) are sufficiently close to that of Li^+ (0.60 Å) to be considered for inclusion in the SEI as defect impurities (Frenkel defects). Reference to Table 1 shows that only Si and Sn are present in the outer β layer after discharge and, as they must have negotiated the SEI during discharge, we assume that there is no reason to suppose that they are not present in the SEI very soon after the start of discharge, thus contributing to the electrical conductivity of the crystals composing the SEI.

We mentioned above that the Fluka sample exhibited the smallest increase in Si levels present in the β LiCl layer after discharge. This is confusing as the Fluka sample has the highest Si concentration of all the lithium samples tested. At both 20 °C and 70 °C, however, the Fluka sample had the highest Si concentrations in the LiCl film stored in electrolyte, so the results only show that the difference between the Si levels in the "stored" and "post-discharged" LiCl films is negligible for the Fluka lithium. It would appear that at both temperatures the Si concentrations in the β LiCl reached an equilibrium maximum before discharge and could not be increased during discharge.

The XPS analysis of the passivating layer is not representative of the SEI, but is an analysis of the outer, more porous β film, which probably presents very little hindrance to ionic transport. Nevertheless, we consider it significant that Sn was not found in the β layer in lithium which had been stored in electrolyte, but was detected in all samples (β layer) after discharge at 20 °C and at 70 °C. Clearly, Sn may contribute significantly to the electronic conductivity of the SEI, as the XPS analysis demonstrates the mobility of Sn^{4+} through both α and β LiCl films during discharge.

Failure of the anode due to passivation is not normally recognised in lithium batteries, probably because it outperforms the carbon cathode. There have been relatively few reports in the literature of premature battery failure due to anode passivation but, for $SOCl_2$ batteries, some cases [22, 23] have been documented. This represents a safety hazard as it constitutes an undesirable failure mode with unused lithium metal remaining in an apparently fully discharged cell. The use of carbon materials other than SAB with improved performance [24, 25] may, in future, serve to demonstrate this hitherto little recognised failure of the lithium anode. Clearly, if high capacity carbon materials are used in commercial cells in preference to SAB, a serious attempt must be made to determine the maximum acceptable impurity levels in the anode to ensure that this cell component does not experience premature failure.

The anomalously high on-load voltage for the Fluka lithium sample may be due to the fortuitous presence of various impurities. The specific Li^+ conductivity of the LiCl film controls the SEI resistance which determines cell performance. The concentrations of higher valent ions such as Al^{3+} and Mg^{2+} are generally known to be proportional to the specific Li^+ conductivity and, as the Fluka lithium sample is particularly rich in these two impurities, they may account for its high on-load voltage. Indeed, a case may exist for the intentional doping of lithium (or the SEI) intended

for lithium/oxyhalide battery manufacture, with suitable impurity cations. For the other lithium samples tested, Sn and Si appear to be more mobile in the SEI and are readily detected in the outer porous layer by XPS. The Lithco lithium sample, which exhibits the best on-load voltage both at 20 °C and at 70 °C, has, in general, the highest Si and Sn levels detected in the porous LiCl layer after discharge.

Conclusions

(i) Lithium samples from different commercial sources exhibit variable performance in test cells due to the electronic conductivity, permeability, and mechanical strength of the LiCl passivating film.

(ii) Load voltages are controlled by the thickness and electronic conductivity of the LiCl passivating layer, that can apparently be influenced by impurities, the most important of which we consider to be Sn and Si, present in the bulk lithium.

(iii) The discharge time of cells fabricated from the different lithium samples is associated with the impurity concentration of sodium in the anodes.

(iv) Surface concentrations of impurities are marginally higher in all "pure" lithium samples, but this surface excess is rapidly depleted in the material which is essentially homogeneous.

References

1 J. R. Driscoll, G. L. Holleck and D. E. Toland, *Proc. 27th Power Sources Symp., 1976*, The Electrochemical Society, Pennington, NJ, p. 28.
2 S. D. James, *J. Power Sources, 10* (1983) 105.
3 S. D. James, *Proc. Lithium Battery Symp., 1983*, Vol. 84-1, The Electrochemical Society, Pennington, NJ, p. 18.
4 E. Peled and H. Yamin, *Proc, 28th Power Sources Symp., Atlantic City, NJ, 1978*, The Electrochemical Society, Pennington, NJ, pp. 237 - 241.
5 E. Peled, in J. P. Gabano (ed.), *Lithium Batteries*, Academic Press, London, 1983.
6 M. Babai and J. Bineth, *J. Power Sources, 9* (1983) 295.
7 A. N. Dey, *Electrochim. Acta, 21* (1976) 377.
8 F. Alessandrini, B. Scrosati, F. Croce, M. Lazzari and F. Bonino, *J. Power Sources, 9* (1983) 289.
9 A. Leef and A. Gilmour, *J. Appl. Electrochem., 9* (1979) 663.
10 A. N. Dey, *Thin Solid Films, 43* (1977) 131.
11 Y. Avigal and E. Peled, *J. Electroanal. Chem., 76* (1977) 315.
12 C. D. Wagner, W. M. Riggs, L. E. Davis, J. F. Moulder and G. E. Muilenberg, *Handbook of X-ray Photoelectron Spectroscopy*, Perkin-Elmer Corp., Minneapolis, MN, 1979.
13 W. P. Kilroy and C. R. Anderson, *J. Power Sources, 9* (1983) 397.
14 C. R. Walk, in J. P. Gabano (ed.), *Lithium Batteries*, Academic Press, London, 1983.
15 R. G. Keil, T. N. Wittberg, J. R. Hoenigman and R. C. McDonald, *Proc. 29th Power Sources Conf., Atlantic City, NJ, 1981*, The Electrochemical Society, Inc., Pennington, NJ, pp. 132 - 135.

16 S. Hofman, *Surf. Interface Anal., 9* (1986) 3.
17 D. Lipinsky, R. Jede, O. Ganshow and A. Benninghoven, *J. Vac. Sci. Technol., A3* (1985) 2007.
18 M. P. Seah, *Thin Solid Films, 81* (1981) 279.
19 A. J. Hills, personal communication.
20 R. W. Holmes, *Proc. 29th Power Sources Conf., Atlantic City, NJ, 1981*, The Electrochemical Society, Inc., Pennington, NJ, pp. 323 - 333.
21 J. W. Boyd, *J. Electrochem. Soc., 134* (1987) 18.
22 A. N. Dey, *Electrochim. Acta, 21* (1976) 855.
23 D. J. Salmon, M. E. Adamczyk, L. L. Hendricks, L. L. Abels and J. C. Hall, *Proc. Lithium Battery Symp., 1981*, Vol. 81-4, The Electrochemical Society, Inc., Pennington, NJ, p. 64.
24 K. A. Klinedinst, *J. Electrochem. Soc., 132* (1985) 2044.
25 K. A. Klinedinst, *U.S. Pat. 4, 461, 814* (1984).